Extended Abstracts of the 1996 International Conference on Solid State Devices and Materials, Yokohama, 1996, pp. 655-657

Improvement on Coupling Efficiency for Passive Alignment of Stacked Multi-Fiber Tapes to a Vertical-Cavity Surface-Emitting Laser Array

Yasuhiro KOBAYASHI, Kenichi MATSUDA, Toyoji CHINO,
Takayuki YOSHIDA, and Kenzo HATADA

Semiconductor Research Center, Matsushita Electric Industrial Co., Ltd.
3-1-1 Yagumo-Nakamachi, Moriguchi, Osaka 570, Japan

High-efficiency coupling of stacked multi-fiber tapes to a vertical-cavity surface-emitting laser (VCSEL) array is demonstrated. Three fiber tapes each of which includes four multimode fibers are coupled to a 4 × 3 VCSEL array by simply inserting fibers into guiding holes fabricated on the back side of the substrate. Mirror-smooth floors of the holes are formed by electron cyclotron resonance reactive ion beam etching, which results in great improvement on coupling efficiency. The average of measured coupling efficiencies is 81.3%.

1. INTRODUCTION

Vertical-cavity surface-emitting lasers (VCSELs) are attractive candidate for low-cost and high-performance parallel optical transmitter modules[1]. Since the VCSEL has an advantage of low cost due to their high productivity, simple and efficient coupling of optical fibers to the VCSELs comes to an essential technology to realize the practical modules. High coupling efficiency more than 70% for 10 × 10 multimode fiber (MMF) bundle to a VCSEL array was demonstrated by using active alignment[2]. This coupling was butt coupling of the bundle against a front surface of the VCSEL array. On the other hand, we demonstrated simple passive alignment of stacked multi-fiber tapes to a 4 × 3 VCSEL array with back-side guiding holes[3]. This module was composed of minimal components, which are the VCSEL array chip, optical fiber tapes and a Si submount. The coupling efficiency of 35% on average was obtained by just inserting fibers into the guiding holes which were precisely aligned to the VCSEL array on the front side.

In this paper, we have greatly improved coupling efficiency by refining the process to open the guiding holes. Quite smooth and mirror-like floors are obtained by electron cyclotron resonance reactive ion beam etching (ECR-RIBE). It results in a coupling efficiency of 81.3% on average.

2. STRUCTURE AND FABRICATION

The schematic cross-section of the assembled SEL chip with the multi-fiber tapes is shown in Fig. 1. The SEL has a 0.98-μm InGaAs/GaAs single quantum well (SQW) sandwiched by two 24.5-pair GaAs/AlAs distributed Bragg reflectors (DBRs). Both DBRs have graded layers composed of short period superlattices at their each heterointerface. The top DBR is n-type and the bottom is p-type. N-type contact metal is AuGe/Ni. A cathode microbump is formed by the side of each SEL mesa and electrically connected to the SEL through Ti/Au line. An anode microbump is formed outside of the SEL array. Since p-n junction in the anode microbump is short-circuited, the anode is electrically connected to the p-DBR.

This common-anode SEL[4] has several advantages. It is preferable in designing the driving circuit because the cathode of the SEL can be connected to the collector of an n-p-n transistor or to the drain of an n-channel FET. Furthermore, it is suitable for integration with a heterojunction bipolar transistor (HBT)[5].

The guiding holes are formed on the back side of the substrate and each hole is precisely aligned to a SEL mesa on the front side. The holes have diameter of 130 μm and depth of ~15 μm. The substrate is diced to the chip, and the chip is bonded to a Si submount in face-down manner. A 4 × 3 fiber array consisting of three multi-fiber tapes with four GI-50/125 fibers is inserted into the guiding holes as shown in Fig. 2.

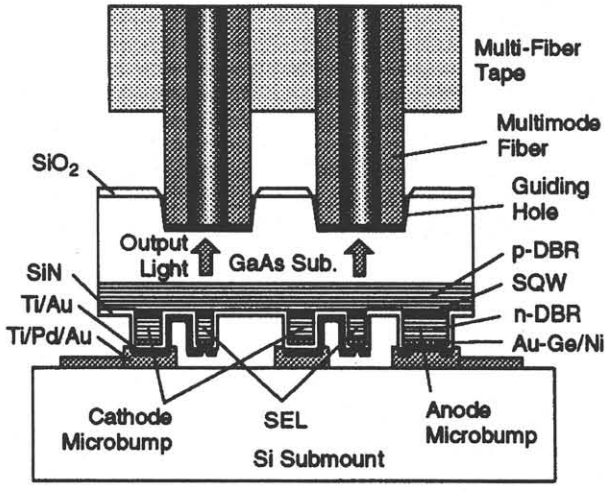

Fig. 1. Schematic cross-section of a surface-emitting laser (SEL) array coupled with multi-fiber tapes into the back-side guiding holes.

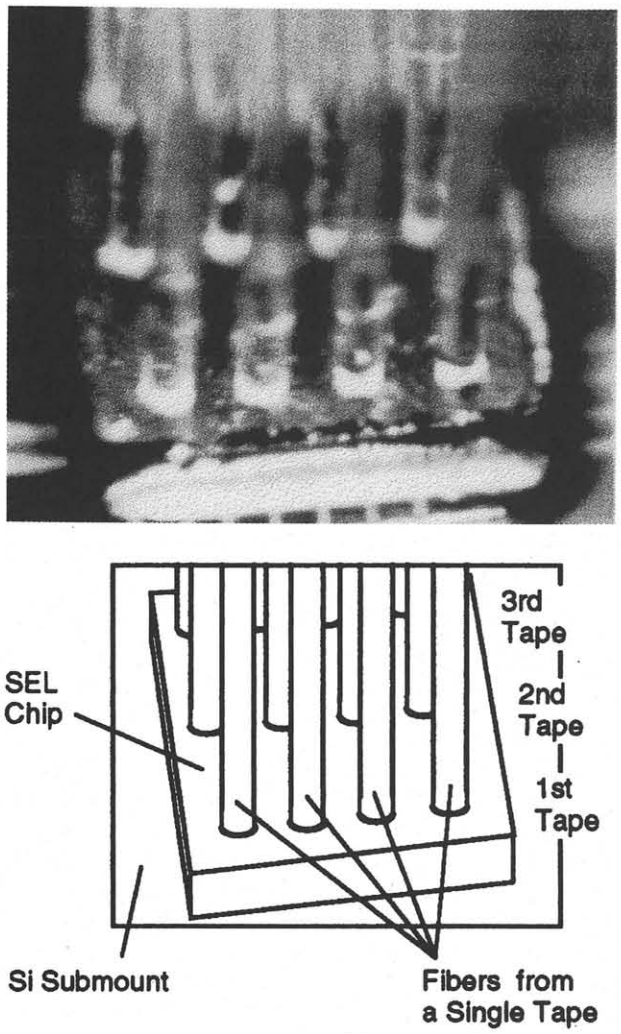

Fig. 2. Photomicrograph and its schematic drawing of optical fibers inserted into guiding holes.

All epitaxial layers are grown by molecular beam epitaxy (MBE). Both the SEL mesas and the microbumps are simultaneously formed by reactive ion etching (RIE). This etching is stopped just under the active layer to make the common-anode configuration. After the mesas and microbumps are covered with SiN, Ti/Au line are formed.

The guiding holes on the back side are aligned to the SEL mesa on the front side with a double-side mask aligner by which both sides of a wafer can be observed simultaneously. Eching of the holes is made by electron cyclotron resonance reactive ion beam etching (ECR-RIBE) with Cl_2 where SiO_2 is used as a mask. The formation of the guiding holes is refined to obtain the high-efficiency coupling. The previous holes were formed by RIE and had rough bottom surface like ground glass as shown in Fig.3(a). It scattered the laser beam and degraded the coupling efficiency. On the other hand, ECR-RIBE allows us to make smooth surface because of higher ion density and stronger sputter effect. An optimized etching gives the mirror-like surface as shown in Fig. 3(b).

The SEL chip is bonded to the Si submount by microbump bonding (MBB) method[6]. The microbumps are alined and pressed to the Ti/Pd/Au pads on the submount, which has a few drops of resin. The resin between both electrodes is pushed out, and contact between electrodes is maintained by shrining stress of the resin cured with UV rays.

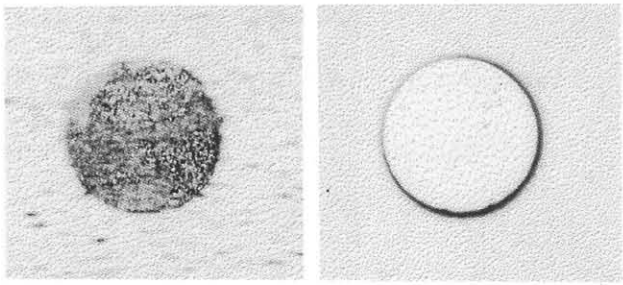

(a) (b)

Fig. 3. Photomicrographs of bottom surfaces etched by (a) RIE and (b) ECR-RIBE. The surface formed by ECR-RIBE is quite smooth like a mirror.

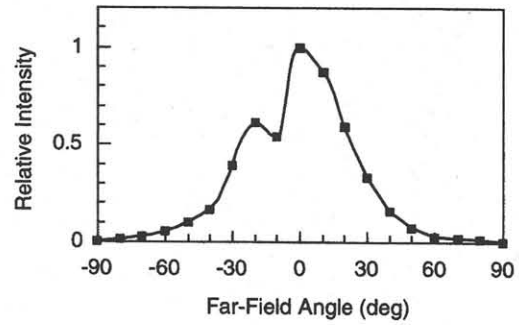

(a)

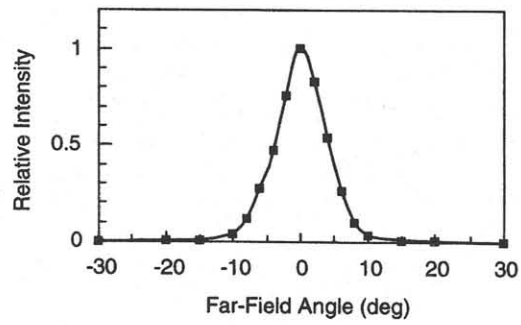

(b)

Fig. 4. Far-field patterns of a SEL beams through guiding holes formed by (b) RIE and (c) ECR-RIBE.

3. CHARACTERISTICS

Far-field patterns of the SEL beams through the guiding holes are shown in Fig. 4. A wide and asymmetric far-field pattern is shown in Fig. 4(a). This is because the SEL beam is scattered at the rough bottom surface formed by RIE shown in Fig. 3(a). On the other hand, a very narrow and symmetric far-field pattern is obtained when the guiding holes are etched by ECR-RIBE as shown in Fig. 4(b). The FWHM of the far-field pattern is 8.0 degrees. This is due to the quite smooth surface shown in Fig. 3(b). It is considered that this beam is narrow enough to obtain high coupling efficiency when the fibers are inserted into the guiding holes.

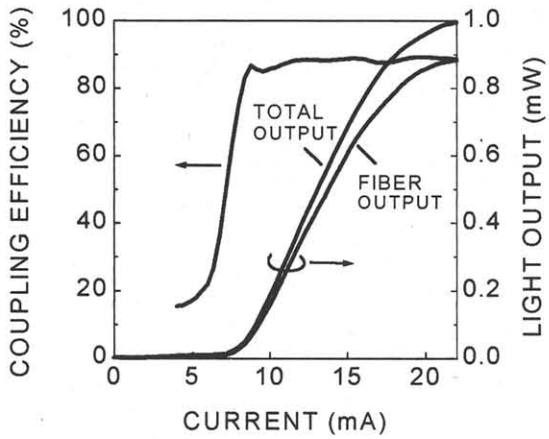

Fig. 5. Coupling efficiency and output power characteristics.

For a SEL in the array, the coupling efficiency is plotted in Fig. 5 in association with total and fiber output powers. The measurement was done under continuous wave (CW) condition. A diameter of the SEL is 30 μm. The fiber output of 0.88 mW is obtained at the current of 22 mA and the efficiency is around 90%. This is a result for passive alignment, that is, simply inserting a fiber into the guiding hole. Active alignment to a lasing SEL shows no difference in efficiency from that of the passive alignment. For a 4 × 3 SEL array, the distribution of the efficiencies is plotted in Fig. 6. These SELs have a diameter of 14 μm. In the second tape, #3 efficiency is over 100%. It is because the output power of the SEL was increased after fiber coupling though it is not the usual case. In general, the output power are not changed at all or rather degraded due to pressure of fiber insertion. Eliminating this value, the average efficiency is 81.3%. In this fiber coupling, the measurements were done under pulsed conditions because the SEL chip had high series resistance due to abrupt DBRs. Array coupling for the SEL chip with the graded DBRs is now under estimation and efficiencies comparable to the results shown in Fig. 6 can be expected.

4. SUMMARY

Simple and efficient coupling of a stacked multi-fiber tapes to a common-anode SEL array with back-side guiding holes has been demonstrated. The obtained coupling efficiency is

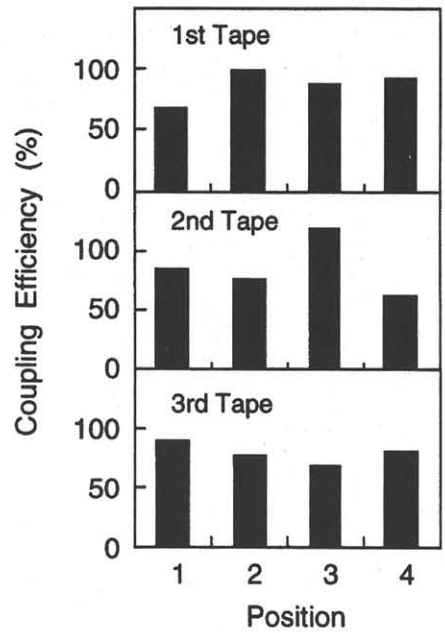

Fig. 6. Distribution of coupling efficiencies in passive alignment of multi-fibers to the 4×3 SEL array.

81.3% on average. The high efficiency results from the mirror-like bottom surface of the guiding holes etched by ECR-RIBE.

References

[1] K. Iga, F. Koyama, and S. Kinoshita, IEEE J. Quantum Electron. **24**(1998) 1845.

[2] E. Zeeb, B. Möller, G. Reiner, M. Ries, T. Hackbarth, and K. J. Ebeling, IEEE J. Select. Topics **QE1**(1995) 616.

[3] K. Matsuda, T. Chino, T. Yoshida, Y. Kobayashi, and K. Hatada, in Tech. Dig. IEDM (Washington, DC, 1995) 587.

[4] H. Adachi, Y. Kobayashi, T. Chino, and K. Matsuda, Japan. J. Appl. Phys. **33**(1994) 836.

[5] T. Chino, Y. Kobayashi, and K. Matsuda, in Tech. Dig. IEDM (Washington, DC, 1993) 921.

[6] K. Hatada, H. Fujimoto, T. Ochi, Y. Ishida, IEEE Trans. Comp., Hybrids, Manuf. Technol **13**(1990) 521.